https://ntrs.nasa.gov/search.jsp?R=19690004311 2018-07-25T22:23:11+00:00Z

N 69 13643
NASA CR 97911

CASE FILE COPY

DEC 1968
RECEIVED
NASA STI FACILITY
INPUT BRANCH

ENERGY DEPOSITION IN MICROSCOPIC VOLUMES BY HIGH-ENERGY PROTONS*

Jerald W. Hilbert and Norman A. Baily+

Department of Radiology, Emory University, Atlanta, Georgia 30322

3 copies submitted
18 manuscript pages
6 figures
1 table

---

*This work was partially supported by the National Aeronautics and Space Administration, Grant No. NGR-11-001-026.

+Present address: Department of Radiology, University of California, San Diego.

Proposed Running Head: PROTON ENERGY DEPOSITION

Address for Proofs: Dr. J. W. Hilbert
Department of Radiology
402 Woodruff Building
Emory University
Atlanta, Georgia 30322

Jerald W. Hilbert and Norman A. Baily

Energy Deposition in Microscopic Volumes
by High-Energy Protons

Radiation Res. __, pp. ___-___, ____.

ABSTRACT

Measurements of the frequency distributions of the energy deposited as the result of the passage of high-energy protons through microscopic volumes of biological interest present some unique problems. A method is described which permits the determination of such distributions in arbitrarily shaped volumes having dimensions equivalent to fractions of a micron of unit-density tissue. The method is illustrated for a 1.77 micron diameter tissue sphere, irradiated with 40 MeV protons, and implications to other energies and geometries are made in terms of the generalizations possible from these results. Distributions for various depths in a tissue-like phantom are also presented.

KEY WORDS

Protons

Energy Deposition

Microdosimetry

INTRODUCTION

Investigations of the frequency distributions of the energy deposited in microscopic tissue volumes traversed by ionizing particles have become of increasing interest, not only because of their importance in predicting the effects of different types of radiation on complex living systems, but also because of their probable importance in many basic radiobiological studies. The most commonly used measurement technique, introduced by Rossi and Rosenzweig (1), is to simulate spherical tissue volumes, having diameters as small as a fraction of a micron, by a much larger proportional counter having tissue-equivalent walls and a spherical volume filled with a low-pressure, tissue-equivalent gas. An assumption inherent in these measurements is that the ionizing particle flux entering the gas-filled measuring volume of the counter is identical to that which would enter the tissue volume simulated if it were placed at the same point in space. While this condition appears to have been at least approximately satisfied for most reported measurements in neutron or gamma-ray fields, these same techniques have often been applied to measurements in charged particle fields with no explicit recognition of the resultant difficulties in satisfying this condition. This assumption will, in fact, be violated whenever there is a significant change in either the primary or secondary charged particle spectrum over distances comparable to the counter dimensions, an occurrence which is quite often inherent in measurements involving charged particles. Such a perturbation occurs for different reasons in different energy ranges.

This perturbation was first encountered by us in examining the problems involved in making microdosimetric measurements in a 50 MeV

proton beam using a tissue-equivalent spherical proportional counter. This counter had a 5.1 cm diameter sensitive volume and 0.3 cm thick walls composed of Shonka muscle-equivalent plastic (2). The tissue-like filling gas, which flowed through the counter, was an equimolar He-CO_2 mixture, having an electron density of 3.01×10^{23} electrons/g. This compares to 3.31×10^{23} electrons/g for ICRU muscle (3). For measurements concerned only with non-nuclear charged particle interactions, simulation of the electron density of tissue is sufficient. A more complicated simulation is required for measurements of frequency distributions of energy deposition due to very high energy particles, where nuclear interactions become important.

In this relatively low-energy range a significant perturbation of the primary proton energy would occur if one were to attempt to make frequency distribution measurements directly using such an instrument. That is, a monoenergetic parallel beam of protons would see different effective wall thicknesses when impinging upon various portions of the counter, resulting in differential energy losses in the counter wall. This would lead to protons with significantly different energies entering the counter's sensitive volume. For instance, for a parallel beam of 46 MeV protons impinging upon the bare tissue-equivalent proportional counter described above, the protons entering at the extreme edges of the counter would have been degraded in energy to 28.5 MeV, while those passing through the wall at the center of the counter would have an energy of 43.5 MeV. This results in a difference in proton stopping power in the He-CO_2 gas mixture of approximately 46%. This differential energy loss becomes even more significant, of course, if one attempts to place the counter within a phantom. For 46 MeV

protons, for example, with the front surface of the counter as close to the phantom surface as is possible, 17% of the projected area of the counter would be at a depth greater than the range of the protons! This differential wall thickness (or tissue depth for measurements in a phantom) can cause similar difficulties at very high (> 200 MeV) proton energies. Recently measured center line depth dose curves for protons (4) with energies ranging from 300-730 MeV show a steep rise in absorbed dose near the phantom surface, due to buildup of secondary charged particles produced by nuclear interactions. In this higher proton energy range the main problem would not be perturbation of the primary protons but of the secondary charged particle flux since, clearly, for any measurements near the surface (5-10 cm) the differential absorber (or simply wall) thickness would result in differential secondary production and thus lead to a meaningless result. It should be realized that these factors would be even more of a problem for the 4-inch diameter chambers widely used for microdosimetric measurements.

In order to overcome these difficulties inherent in proton microdosimetry, an experimental technique was developed which allows proper determination of the frequency distributions of energy deposition along individual pathlengths, and yields the whole counter (microvolume) response by the proper folding together of the individual partial responses.

EXPERIMENTAL METHOD

The experimental study of proton energy deposition frequency distributions was performed at the University of California at Los Angeles' 50 MeV Sector Focusing Cyclotron. The frequency distributions of energy

deposition due to passage of monoenergetic protons along a single path-length were examined by positioning a small frontal area, 1.5 cm path-length, silicon, lithium-drifted, p-i-n detector directly behind a tissue-equivalent proportional counter and operating them in double coincidence. The resulting coincidence spectra were then due to the passage of essentially monoenergetic protons along a well defined straight line path through the proportional counter. Details of the experimental set-up have been presented previously (5), the only difference in the present set-up being the use of a proportional counter with tissue-equivalent walls as well as a tissue-equivalent filling gas.

The energy calibration of the proportional counter was accomplished by measuring the spectrum of energy depositions along a single pathlength for an accurately determined proton energy, operating the counter at a high enough pressure (600 Torr) that essentially the entire spectrum could be very accurately determined (i.e., the extent of the high-energy-loss tail, which will be seen to be characteristic of such spectra, is reduced and may thus be measured with statistical meaningfulness). This is necessary for an accurate calibration because of the relatively large contribution of the infrequent large energy depositions to the average energy deposited in the volume being investigated. The average energy deposition was then determined by integration of the experimental data and was correlated with the average energy loss, calculated using Barkas and Berger's proton stopping power tables (6), to provide the calibration (the <u>average</u> energy deposition and the <u>average</u> energy loss are equal under conditions of electron equilibrium). The absolute energy calibrations at all other pressures utilized were then obtained by using a collimated (internal) beam of alpha particles to determine the relative

gas gains at these pressures. This direct proton energy-loss measurement at one pressure eliminates the problem of determining an exact value of W, the average energy required to produce an ion pair in the gas mixture.

RESULTS & DISCUSSION

For volumes of the order of cellular magnitudes and smaller, one of the predominant factors influencing the local energy deposition distributions is very often the significant fluctuations of energy-loss experienced by charged particles in passing through "thin" absorbers. Energy-loss distributions in such situations are generally quite markedly asymmetric and characterized by a most probable energy-loss which is significantly less than the mean energy-loss, and a high-energy-loss "tail." It has been shown previously (5) that some general features of the energy-loss distributions for very small mean energy losses (when losses to bound electrons become important) may be adequately described by applying the Blunck-Leisegang resonance collision correction (7) to the Vavilov (8) energy-loss theory. However, it is important to realize that any theory predicting energy-<u>loss</u> distributions for charged particles passing through an absorber with cellular dimensions may in many cases not at all realistically describe the frequency distribution of energy <u>deposited</u> in such a volume, which is of interest from the viewpoint of biological effects. These distributions will only be identical if the absorber thickness is somewhat greater than the range of the maximum energy delta rays which may be produced. If the absorber is so thin that a significant number of delta rays deposit only part of their energy in the absorber thickness, the actual distributions may differ considerably from those theoretically expected, especially in

the high-energy tail region. The distributions measured experimentally using the proportional counter and reported here are, of course, the biologically significant frequency distributions of the energy deposited.

Before discussing the experimental results obtained, a word should be said regarding the simulation, for protons, of a tissue path with the "tissue-like" gas mixture used in the proportional counter. The gas path along a diameter of the proportional counter when it is operated at a pressure of 20 Torr, for example, simulated 1.18 microns of tissue in the sense that the same average energy is lost is traversing the gas path and, because of the approximate equality in electron densities, quite similar frequency distributions of energy-loss are predicted (i.e., if the electron densities were markedly different, the predicted frequency distributions of energy-loss for the same average energy loss would be quite different). The ratio of the mass stopping power of tissue to the mass stopping power of the He-CO_2 gas mixture changes very little in the energy range of interest here (< 3% change from 50 MeV to 2 MeV), so that the "equivalence factor" relating g/cm^2 of He-CO_2 to g/cm^2 of tissue may be taken to be a constant (6). Since the relative mass stopping power of tissue to the He-CO_2 mixture is approximately 1.13 in this range, 1.33×10^{-4} g/cm^2 of He-CO_2 (density of the mixture of 20 Torr pressure x pathlength in the counter) simulates $1.33 \times 10^{-4}/1.13 = 1.18 \times 10^{-4}$ g/cm^2, or 1.18 microns, of unit-density tissue.

A set of measurements were made for a single proton energy to illustrate the method by which the energy deposition distribution in a spherically (or arbitrarily) shaped microvolume may be determined and to explore some of the implications of this method. The frequency

distribution of energy deposition in a complete microvolume is approximated by measuring energy deposition distributions for a series of pathlengths and folding together these distributions on the basis of the relative number of pathlengths of each value seen by a parallel beam of protons incident on the particular volume. The volume most amenable to a simple interpretation is, of course, a sphere which was originally analyzed by Rossi et al. (1). A spherical volume results in a particularly simple distribution of pathlengths, given (for a parallel beam of incident radiation) by $P(x) = {}^{x}/2r^{2}$, where r = sphere radius, and x = pathlength ($0 \leq x \leq 2r$). While there are obviously biological volumes of significance which may be more closely approximated by other shapes, only a spherically shaped volume will be treated in detail here, because of its relative simplicity, and implications to other shapes will be made in terms of the generalizations possible from the spherical example. The procedure for other volumes is, in principal, identical.

Energy deposition distributions were measured at pressures of 30.0, 25.0, 20.0, 15.0, 10.0, and 5.0 Torr for protons with an energy of 40.0 MeV entering the sensitive gas volume of the tissue-equivalent proportional counter. These pressures simulate tissue paths of 1.77, 1.48, 1.18, 0.886, 0.590 and 0.295 microns, respectively. The distributions were obtained using the coincidence requirements described above so that these paths were accurately described. The energy deposition distributions obtained are shown in Figure 1. It will be noted that a set of axes have been provided for these curves which give the absolute probability per keV of a given energy deposition versus the energy deposition in keV. This absolute normalization was obtained by

graphically integrating the distributions and imposing the condition that the area under each curve be equal to 1.00 (i.e., the probability that a proton passing through the given pathlength loses some amount of energy, including zero, is unity). Ideally each experimental distribution should be integrated from zero to the energy of the incident proton (since there is an infinitesimally small probability of the proton losing its entire energy in the counter), or, more realistically, at least to the much smaller energy deposition corresponding to the maximum possible energy transfer to an atomic electron in a single collision ($\simeq$ 89 keV for 40.0 MeV protons). In practice, however, energy events of this magnitude are vanishingly infrequent, and the experimental distributions were integrated in each case to an energy deposition which includes greater than 98% of the possible energy-losses predicted by theory (8). Since some high-energy delta rays may deposit only part of their energy in the counter, the integration will include, if anything, an even greater percentage of all possible energy depositions and, thus, represents a very good approximation of the total area. Probability values are next taken from the normalized curve for each pathlength, using a sufficiently fine energy grid, and are weighted according to the relative number of each such pathlength in a spherical volume, given by $P(x) = x/2r^2$, where the maximum pathlength simulated is set equal to 2r. These weighted values are then added together to yield the probability distribution of energy deposition in the entire spherical microvolume, which in this case has a diameter of 1.77 microns. This procedure, which is quite straightforward in concept, is rather tedious and time-consuming when done by hand; and processing of the data by a computer program is obviously highly desirable for routine use of such a method.

An obvious question relating to this method is how many individual pathlengths must be simulated to obtain a sufficiently accurate approximation to the distribution which would be found in a true spherical microvolume. In order to examine this question, two composite distributions were constructed, one using all six simulated pathlengths, and a second using only three (0.59, 1.18, and 1.77 microns). The resulting distributions are shown in Figure 2. It might be mentioned that greater than 97% of all pathlengths existing in a 1.77 micron diameter sphere are included within the range of simulated pathlengths (0.295 to 1.77 microns). It will first be noted from Figure 2 that a marked discontinuity apparent at $\simeq 0.5$ keV in the curve approximated by only three pathlengths has essentially disappeared in the curve approximated by all six pathlengths. While no absolute quantitative conclusions can be drawn from the limited data available for this comparison, it is probably safe to say, judging from the relative change in the composite distribution upon increasing the number of simulated pathlengths from three to six, that for these experimental distributions the summation of six pathlengths results in a reasonably good approximation to the distribution in the entire microsphere. This conclusion depends, of course, on the widths of the distributions observed for each individual pathlength, the relatively small number of individual pathlengths required in this example being a result of the quite broad individual distributions. For much narrower individual distributions, such as would result if a much larger tissue microsphere were simulated or if the energy losses were more comparable to the proton energy, more individual distributions would be required; while for smaller simulated microspheres or higher energy protons which cases are much more likely

to be of interest for radiobiological applications, only a few would be necessary. It is also possible that the choice of individual pathlengths simulated was not optimum. That is, in any given situation, smaller increments between simulated pathlengths for the more frequent long pathlengths and larger increments for the less frequent pathlengths might result in a better approximation with no increase being required in the total number of pathlengths examined. This whole question of the total number of pathlengths required and their optimum distribution is best examined quantitatively using computer techniques. This is presently being undertaken, and the results will be reported upon completion.

Kellerer (9), in his approximate theoretical treatment of microdosimetric distributions, makes the generalization that, because of the very large statistical fluctuations in energy loss along individual pathlengths, the influence of the track length distribution in a volume is not decisive as long as the mean energy loss is less than several keV, so that similar results should be obtained for all geometries. Exactly what is implied quantitatively by this generalization is a question of interest. Since for the data presented here the mean energy loss in the maximum pathlength (i.e., the diameter) is approximately 2.6 keV, the data seem particularly well suited to examine this question. The simplest and most straightforward shape with which to make a comparison is simply a very thin slab, oriented perpendicular to the incident protons. Such a comparison is made in Figure 3 for a slab shaped volume which has a thickness equal to the average pathlength in the corresponding spherical volume. This average pathlength, for the triangular pathlength distribution which exists in a spherical volume,

is just equal to 2/3 of the spherical diameter, or 1.18 microns. This is the pathlength simulated at 20 Torr, and this measured probability distribution of energy deposition is compared with the distribution for the 1.77 micron sphere in Figure 3. It will be noted that, while both distributions have the same characteristic "low-energy peak, high-energy tail" and, in fact, peak at very close to the same energy, quantitatively they differ greatly. Quantitative predictions relating to biological effects might be expected to differ greatly for the two distributions. Thus, it would appear that Kellerer's generalization needs to be carefully qualified. The third curve displayed in Figure 3 illustrates, for comparison, the triangular energy-loss distribution which would be predicted for the 1.77 micron diameter microsphere if the statistical fluctuations in energy-loss of 40.0 MeV protons were completely ignored (i.e., if it were assumed that every proton passing through the microsphere experienced an energy loss corresponding exactly to that predicted by the proton stopping power). The gross qualitative and quantitative difference of this distribution is obvious.

It is highly desirable that any technique for measuring frequency distributions of energy deposition in microscopic volumes be applicable to measurements at depth in a phantom. Application of the experimental technique described here to measurements in a phantom is based on the fact that the scattering experienced by protons through electronic collisions in their passage through matter is very minimal, resulting in insignificant differences between the proton pathlength and the thickness of absorber traversed (10), as contrasted, for example, with the very tortuous paths of electrons passing through matter. Therefore, when simulating the energy deposition in a microvolume at depth using

this method, it is assumed that protons travel to the depth of the microvolume in essentially straight-line paths and that the contribution of side- and back-scattered protons may thus be neglected.

To illustrate the method, frequency distributions of energy deposition for one simulated pathlength, equivalent to 1.18 microns of tissue, were measured at various depths in Shonka tissue-equivalent plastic for protons with an incident energy of 43.0 MeV. These distributions were obtained by recording the pulse height distributions due to passage of the protons across a diameter of the tissue-equivalent proportional counter, fixed at a pressure of 20 Torr, and placing various thicknesses of tissue-equivalent plastic flush with the front of the counter. Actually, two different types of distributions may be obtained in this manner. For illustrative studies such as the present one, it is of interest to determine such distributions for an essentially monoenergetic incident proton beam, and such distributions are obtained using the coincidence technique already described. In many practical situations, however, biological exposures cannot be performed in a strictly monoenergetic beam. In fact, the procedure used to spread proton beams often results in a spectrum with a not insignificant low energy tail below the main energy peak. A fairly typical proton energy spectrum, measured with the p-i-n semiconductor detector, is shown in Figure 4 (the spectrum is actually that after passage of 44 MeV protons through the two walls of the tissue-equivalent plastic counter). This spectrum shows a considerable fraction of the total proton flux in the low energy tail. Whenever a significant low-energy tail is unavoidable in a biological exposure situation, the corresponding microscopic frequency distribution of absorbed energy which is of interest is obviously that

due to the entire proton spectrum with which the biological sample is irradiated. In such a case, the distribution of energy deposition for a given pathlength may be obtained by simply placing a well designed collimator in front of the proportional counter to produce a pencil-like beam of protons. Distributions of this type were also measured as a function of depth in tissue-equivalent plastic, using a collimator with a window area of $\simeq 0.2$ cm^2.

Figure 5 shows both a coincidence spectrum and a non-coincidence (collimated) spectrum for protons with an incident energy of 43.0 MeV. These spectra, which are typical, were obtained at a depth of 0.20 g/cm^2. It will be noted that the low energy side of the energy deposition peaks are essentially the same, as would be expected, since this part of the peak is due mainly to the numerous protons in the peak of the proton energy spectrum. There are, however, considerably more large energy depositions in the high-energy tail of the distribution produced by the collimated beam due, of course, to the lower energy protons contributing in this case.

Figure 6 shows the frequency distributions obtained using the collimator at depths of penetration of 0.20, 0.60, 1.44, 1.58, and 1.66 g/cm^2 of tissue-equivalent plastic. These distributions have all been arbitrarily normalized to unity at the peak. At a depth of 1.71 g/cm^2, essentially no protons penetrated to the sensitive gas volume. This observation is in good agreement with the calculated range (6) of 1.67 g/cm^2 of tissue-equivalent plastic for 43 MeV protons, and with the 1.36% pathlength straggling (giving $\sigma \simeq 0.02$ g/cm^2) predicted by Janni (10). Some of the experimental parameters are summarized in Table I. The proton energies listed in the table are the

calculated (6) residual energies of an incident 43.0 MeV proton after penetrating to the corresponding depths in tissue-equivalent plastic and are included only to provide a feel for the magnitude of the proton energies corresponding to each spectrum. It will be noted that the distributions retain their characteristic peaked shape even at the largest depths examined, and that the widths of the distributions tend to decrease with depth and then increase again for even greater depths. The widths of the distributions are, of course, determined by the combination of two effects: (1) the fractional width tends to decrease as the mean energy of the incoming protons decreases (increasing the mean energy loss in the cavity), (2) the increasing energy spread of the primary proton spectrum tends to broaden the peak of the distribution. Such an interplay would be extremely difficult to predict theoretically with any confidence.

CONCLUSIONS

It has been shown that application of conventional microdosimetric techniques to measurements in charged particle beams will generally lead to meaningless results. An experimental technique has been described which permits the determination of frequency distributions of energy deposition in arbitrarily shaped volumes having dimensions equivalent to fractions of a micron of unit-density tissue. It has also been shown that for heavy charged particles, which experience minimal scatter, distributions may be measured at depth in a phantom. An illustrative set of measurements indicated that, in general, for measurements in volumes having dimensions which are likely to be of radiobiological interest, relatively few individual pathlengths need be simulated to

approximate the distribution in any given volume. It was also seen that the generalization made by Kellerer, stating that similar distributions will be obtained in all geometries when the mean energy loss is less than several keV, needs to be carefully qualified.

While the experimental procedure outlined here is somewhat complex and is limited to the rather simple case of a parallel beam of charged particles, this is, in fact, the situation most often utilized in basic radiobiological experiments, and this procedure appears to be the only method which will yield meaningful microdosimetric results in these cases. In addition, it may be well to point out that, for a given irradiation geometry, experimental determination of frequency distributions of energy deposition for a range of individual pathlengths yields sufficient data to permit simulation of microdose distributions in arbitrarily shaped microvolumes of various sizes. Finally, while this procedure would not be practical for making routine measurements for protection purposes, there does not appear presently to be any method which can routinely give meaningful microdosimetric measurements when charged particles are involved. The instrument development problem for "in air" protection measurements is, of course, to reduce the chamber wall thickness until its perturbing effect is minimal, a criteria which depends upon the charged particle type and its energy. The difficulties inherent in "in phanta" measurements for charged particles are much more complex, and a simple solution to this problem is not obvious. It should be obvious, however, from the considerations presented here, that increasing the wall thickness to simulate depth doses, as has sometimes been suggested, would be a very poor approach for any general situation involving charged particles.

REFERENCES

1. H. H. Rossi and W. Rosenzweig, A device for the measurement of dose as a function of specific ionization. Radiology 64, 404-411 (1955).

2. F. R. Shonka, J. E. Rose, and G. Failla, Conducting plastic equivalent to tissue, air and polystyrene. Proc. of the 2nd U.N. Inter. Conf. on the Peaceful Uses of At. Energy, 21, 184-187, Geneva (1958).

3. Report of the International Committee on Radiological Units and Measurements (ICRU), Natl. Bur. Std. (U.S.) Handbook 84, (1959).

4. R. L. Tanner, N. A. Baily and J. W. Hilbert, High-energy proton depth-dose patterns. Rad. Res. 32, 861-874 (1967).

5. J. W. Hilbert, N. A. Baily and R. G. Lane, Statistical fluctuations of energy deposited in low-atomic-number materials by 43.7-MeV protons. Phys. Rev. 168, 290-293 (1968).

6. W. H. Barkas and M. J. Berger, Tables of energy losses and ranges of heavy charged particles. Studies in Penetration of Charged Particles in Matter, NAS-NRC Publ. No. 1133, 103-172 (1964).

7. O. Blunck and S. Leisegang, Zum energieverlust schneller elektronen in dünnen schichten. Z. Physik 128, 500-505 (1950).

8. P. V. Vavilov, Ionization losses of high-energy heavy particles. Zh. Exper. Teor. Fiz. 32, 920-923 (1957). Transl. JETP. 5, 749-751 (1957).

9. A. M. Kellerer, Microdosimetry and the theory of straggling. Report on Second Panel on Bioph. Asp. Rad. Qual., I.A.E.A., Vienna (in press).

10. J. F. Janni, Calculation of energy loss, range, path-length, straggling, multiple scattering, and the probability of inelastic nuclear collisions for 0.1 to 1000 MeV protons. AFWL-TR-65-150, Air Force Weapons Lab., New Mexico (1966).

Table I

Summary of Microscopic Energy Deposition Parameters for a 1.18 Micron Simulated Tissue Path (E_o = 43.0 MeV).

Depth in Tissue-Equivalent Plastic	Residual Energy of Incident 43 MeV Proton	Peak Width
g/cm^2	MeV	% FWHM
0.20	40.2	150
0.60	33.5	140
1.44	14.4	109
1.58	8.2	117
1.66	< 3[a]	133

[a]Range of 43 MeV Protons is $\simeq$ 1.67 g/cm^2 of Tissue-Equivalent Plastic.

FIGURE CAPTIONS

Figure 1. Probability distributions of energy deposition due to 40.0 MeV protons passing through various simulated tissue paths. Tissue path in microns: A = 0.295, B = 0.590, C = 0.886, D = 1.18, E = 1.48, F = 1.77.

Figure 2. Probability distribution of energy deposition due to 40.0 MeV protons in a 1.77 micron diameter tissue microsphere. Curve A produced by summation of six pathlengths; curve B by summation of three pathlengths.

Figure 3. Various probability distributions of energy deposition, due to 40.0 MeV protons. A is in 1.18 micron individual pathlength; B is in simulated 1.77 micron diameter tissue microsphere; C is theoretical distribution which would result if there were no statistical fluctuations of energy loss.

Figure 4. Typical energy spectrum of spread proton beam (44 MeV beam after passage through $\simeq 0.40$ g/cm^2 of tissue-equivalent plastic).

Figure 5. Energy deposition distributions in simulated 1.18 micron tissue paths due to 43.0 MeV protons which have penetrated to a depth of 0.20 g/cm^2 in tissue-equivalent plastic. A = coincidence spectrum. B = collimated beam spectrum.

Figure 6. Energy deposition distributions in simulated 1.18 micron tissue paths situated at various depths in tissue-equivalent plastic. The incident proton spectrum had its peak at 43.0 MeV. Depths in g/cm^2 of tissue-equivalent plastic: A = 0.20, B = 0.60, C = 1.44, D = 1.58, E = 1.66.

Rad. Research
Hilbert & Baily
Figure 1

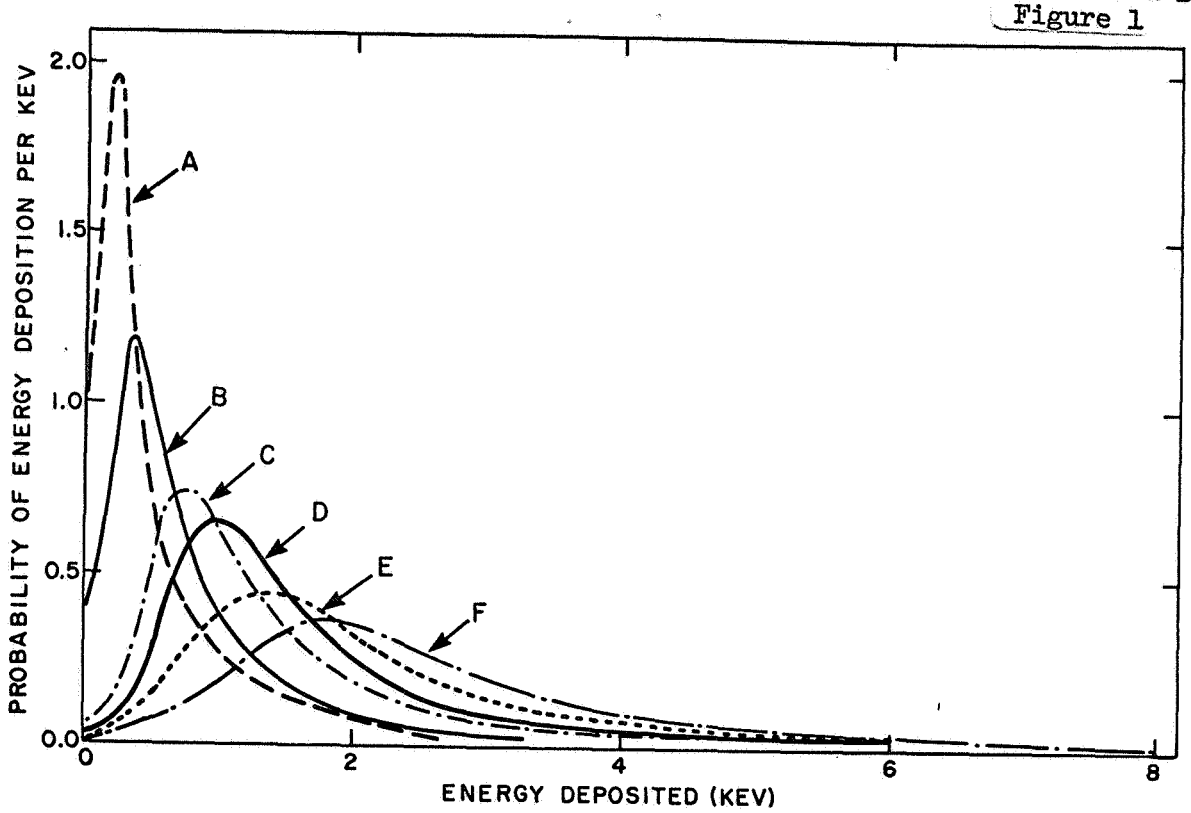

Rad. Research
Hilbert & Baily
Figure 2

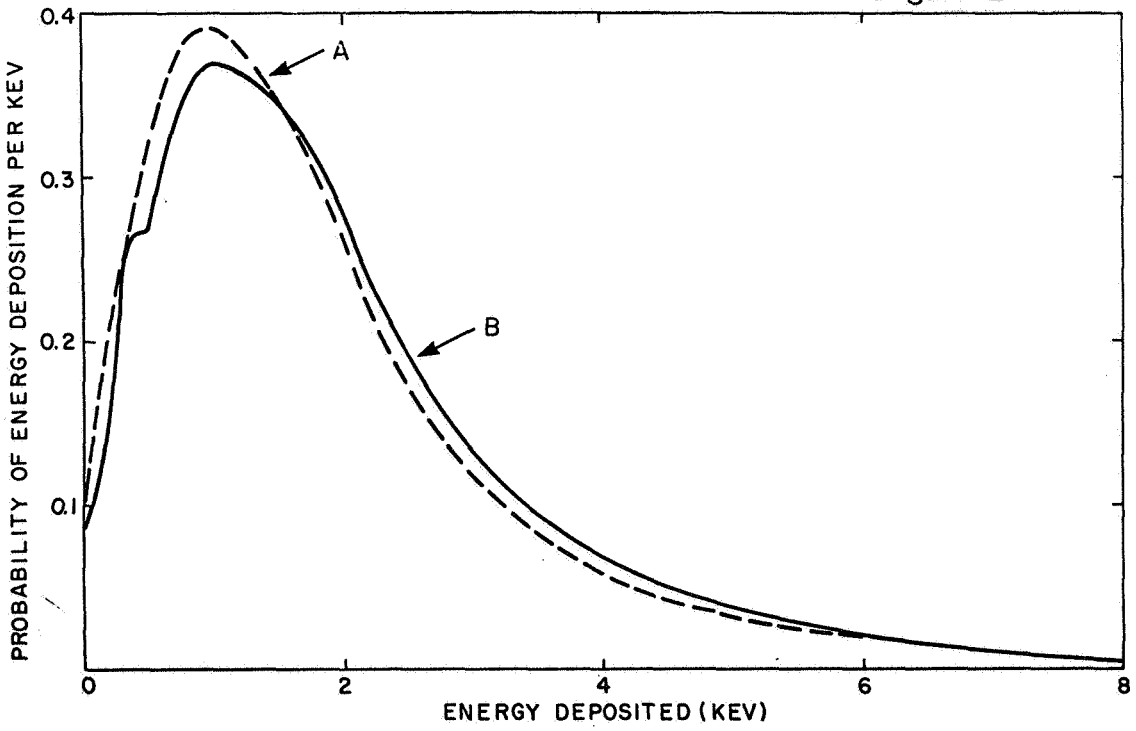

Rad. Research
Hilbert & Baily
Figure 3

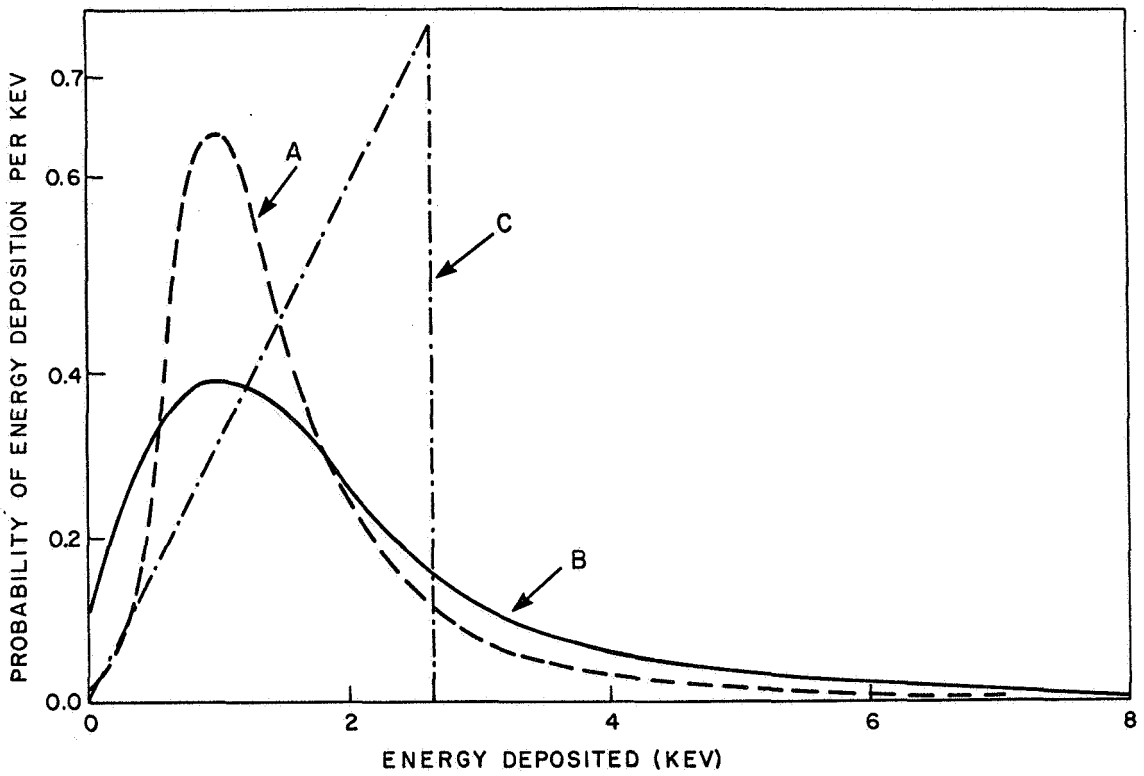

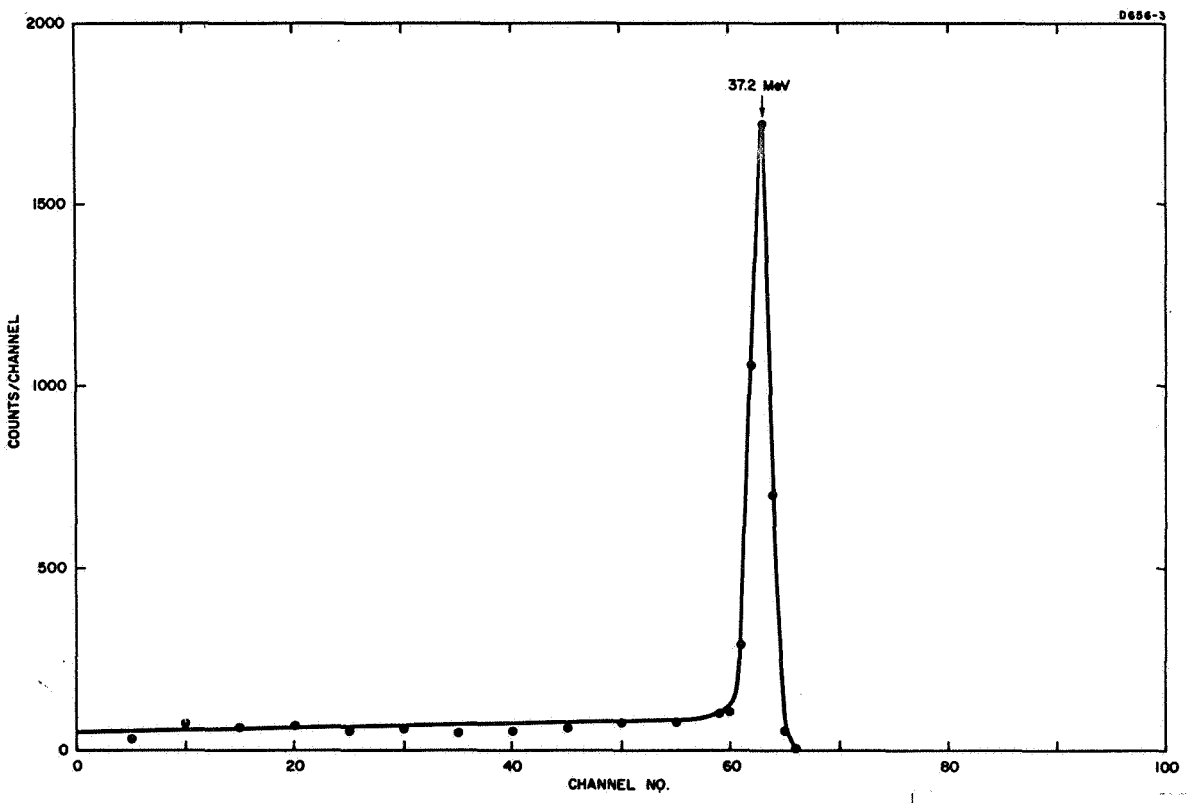

Rad. Research
Hilbert & Baily
Figure 4

Rad. Research
Hilbert & Baily
Figure 5

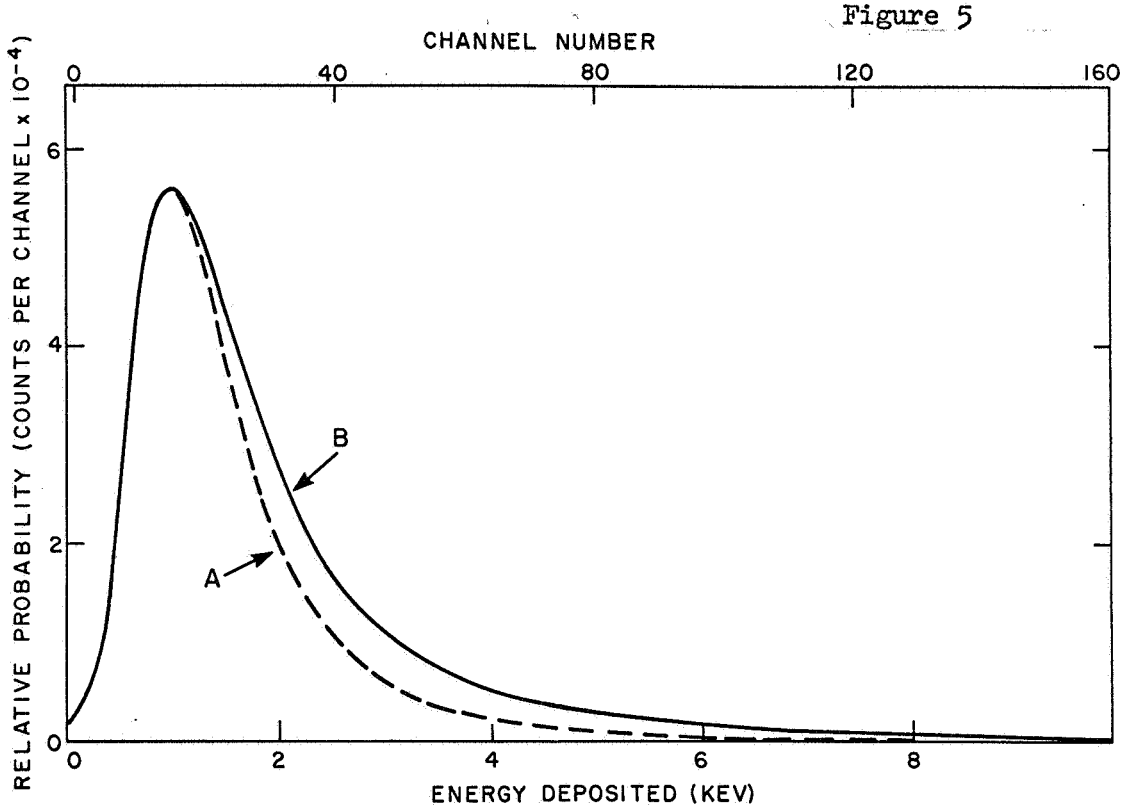
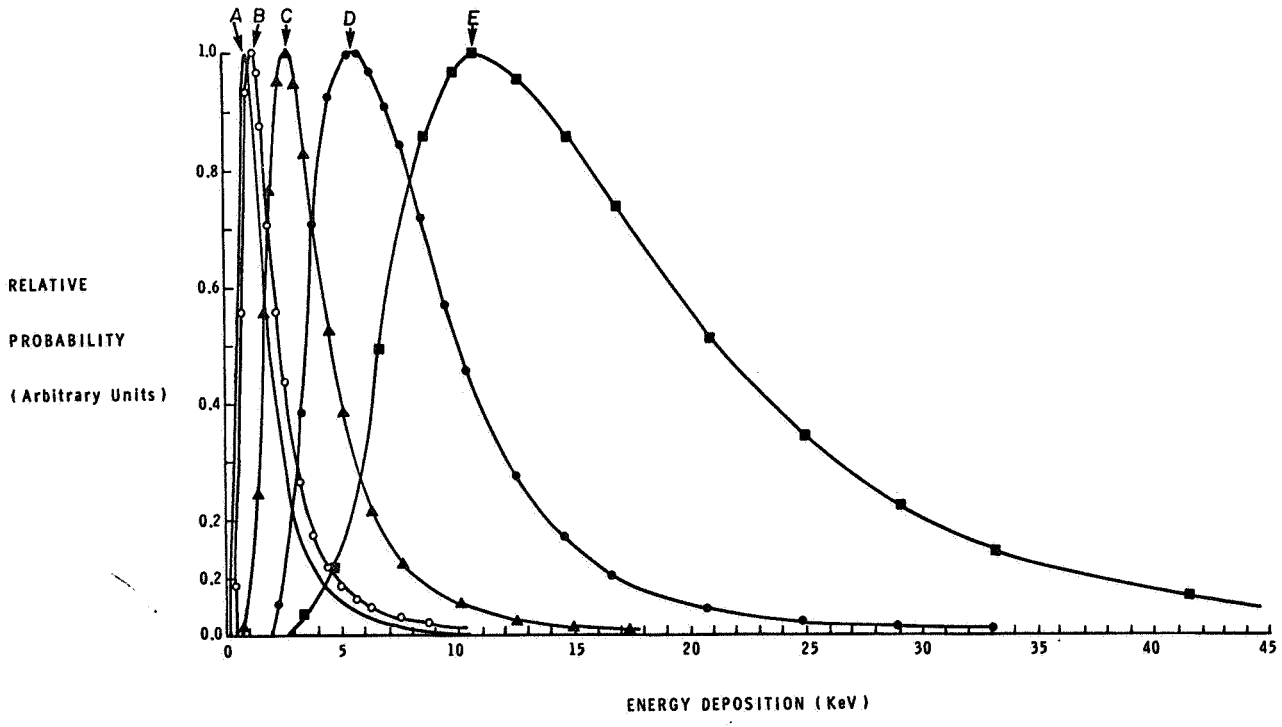
Rad. Research
Hilbert & Baily
Figure 6